GEOPHYSICAL RESEARCH LETTERS, VOL. 17, NO. 6, PAGES 745-748, MAY 1990

A CURRENT DISRUPTION MECHANISM IN THE NEUTRAL SHEET: A POSSIBLE TRIGGER FOR SUBSTORM EXPANSIONS

A. T. Y. Lui, A. Mankofsky, C.-L. Chang,
K. Papadopoulos and C. S. Wu

Abstract. A linear analysis is performed to investigate the kinetic cross-field streaming instability in the Earth's magnetotail neutral sheet region. Numerical solution of the dispersion equation shows that the instability can occur under conditions expected for the neutral sheet just prior to the onset of substorm expansion. The excited waves are obliquely propagating whistlers with a mixed polarization in the lower hybrid frequency range. The ensuing turbulence of this instability can lead to a local reduction of the cross-tail current causing it to continue through the ionosphere to form a substorm current wedge. A substorm expansion onset scenario is proposed based on this instability in which the relative drift between ions and electrons is primarily due to unmagnetized ions undergoing current sheet acceleration in the presence of a cross-tail electric field. The required electric field strength is within the range of electric field values detected in the neutral sheet region during substorm intervals. The skew in local time of substorm onset location and the three conditions under which substorm onset is observed can be understood on the basis of the proposed scenario.

Introduction

The initiation of the expansion phase of a magnetospheric substorm is generally considered to involve a process by which the near-earth portion of the cross-tail current in the magnetotail is drastically reduced or disrupted. The radial extent of current disruption has been estimated quantitatively for a small substorm to be $\sim 3.5\ R_E$ in the innermost portion of the current sheet [Lui, 1978]. The tearing instability has been discussed extensively in the literature as one possible candidate (see, Coroniti, 1985). Another possibility is the lower hybrid drift instability (LHDI) (e.g., Papadopoulos, 1979) which has been proposed to account for the broadband electrostatic noise in the plasma sheet boundary layer [Huba et al., 1978]. However, this mode is stabilized by the high value of plasma beta near the neutral sheet [Huba and Papadopoulos, 1978].

Recent measurements on ISEE indicate lower hybrid waves (LHW) present even in the neutral sheet [Cattell and Mozer, 1987], which suggests a need to reexamine the generation of LHW in the neutral sheet and its implications to substorm models. In this paper, we consider LHW excitation in the neutral sheet by the kinetic cross-field streaming instability (KCSI) discussed previously in connection with the Earth's bow shock [Wu et al., 1984; Winske et al., 1985]. The KCSI and LHDI can then be combined and applied to the entire plasma sheet. The paper concludes with a discussion of the possible implications of the LHW excitation in the neutral sheet to substorm expansion onset.

Paper number 90GL00951
0094-8276/90/90GL-00951$03.00

Instability Analysis and Implications

There are several observed features in the magnetotail leading up to substorm expansion. Prior to the onset, the magnetic field configuration in the near-earth plasma sheet becomes very tail-like. The plasma sheet is thinned to the extent that the ions become unmagnetized in the neutral sheet region when their gyroradii are larger than the field gradient scale length. Kaufmann [1989] has noted that an integrated current density of 300 mA/m is required to create tail-like field configuration near the geosynchronous altitude. If the near-earth plasma sheet is thinned to $0.5\ R_E$ at this time, then the average current density is $0.1\ \mu A/m^2$. For a number density of $0.3\ cm^{-3}$, the relative drift between electrons and ions is 2000 km/s, corresponding to $\sim 10\ v_A$ for B = 5 nT. This will give rise to a significant growth of the KCSI as will be shown later (Figure 2).

We suggest that current disruption in the tail at substorm expansion onset is due to the combined effect of the KCSI in the neutral sheet and the LHDI outside the neutral sheet. Figure 1 illustrates this idea and the coordinate system used in the KCSI calculation. The cross-field drift for the KCSI arises from ions becoming unmagnetized in the neutral sheet (executing Speiser [1965] orbits) and undergoing acceleration in a cross-tail electric field. On the other hand, the free energy source for the LHDI comes from the diamagnetic current associated with a density gradient which is increased considerably by plasma sheet thinning prior to substorm onset. Since the LHDI has already been discussed extensively [Huba et al., 1977], we shall focus on the KCSI in the neutral sheet.

The dispersion equation under consideration is basically the same as that given by Wu et al. [1983] (see the appendix) who have shown that when the ion beta β_i is large, the growth rate γ of the unstable mode is given as

$$\gamma/\omega_r = -\pi^{1/2} \sin^2\theta \left[\xi_i/\beta_i + 0.5\ \beta_e \xi_e \exp(-\xi_e^2)\right] \quad (1)$$

where $\theta = \cos^{-1}(\hat{k}\cdot\hat{B})$ and ω_r is the real frequency given by the approximate whistler dispersion relation $\omega_r \simeq k^2c^2 \cos\theta/\omega_{pe}^2$. The other parameters are defined in the appendix. It can be seen that (1) the growth rate diminishes as θ approaches zero, (2) the KCSI can set in when the drift speed v_o is sufficiently large such that the electron Landau damping is overcome by the ion contribution to growth, and (3) the growth rate decreases when the ion beta increases.

We have solved Eq. (A1) numerically with a dispersion solver benchmarked by solutions given in Wu et al. We adopt $n_e = n_i = 0.3\ cm^{-3}$, $T_i/T_e = 10$, $T_i = 2$ keV, and B_z

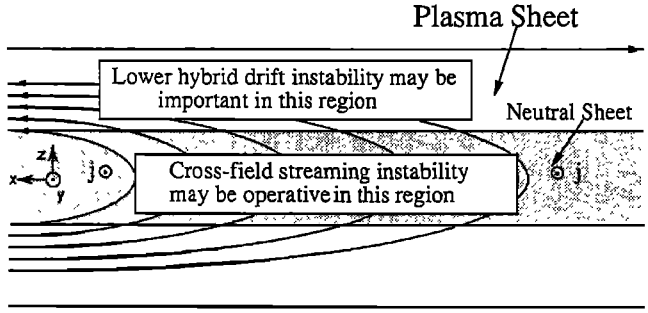

Figure 1. A schematic diagram to illustrate the suggestion that both the KCSI (operating in the neutral sheet) and the LHDI (operating outside the neutral sheet) play important roles in triggering substorms.

= 5 nT for the neutral sheet [Huang et al., 1989]. These parameters give a plasma beta $\beta_i \simeq 10$, $\omega_{pe}/\Omega_e \simeq 35$ and the Alfvén speed $v_A \simeq 200$ km/s. Previous studies of this instability dealt with plasma regimes with $\beta \lesssim 1$. The plasma beta in our situation is about an order of magnitude higher.

Figure 2a shows the wave frequency and growth rate maximized over both the normalized wavenumber $k\rho_e$ and the propagation angle θ for drift speeds ranging from about 2.5 v_A to 20 v_A. The normalization for ω and γ is the lower hybrid frequency $\omega_{lh} = \omega_{pi}/(1 + \omega_{pe}^2/\Omega_e^2)^{1/2}$, which is about 20 rad/s in our case. Growth is significant at drift speed just below 2.5 v_A. Both the frequency and the growth rate become larger with increasing drift speed. At $v_o/v_A = 5$, 10, 20, we find $\omega/\omega_{lh} \simeq 0.13$, 0.42, 1.26 and $\gamma/\omega_{lh} \simeq 0.0072$, 0.032, 0.104 (corresponding to an e-folding time of about 43 s, 9 s, 3 s), respectively. The growth rates should be considered as lower limits since Chang and Wong [1989] have recently shown that the inclusion of electromagnetic response of ions in high β regime can enhance considerably the growth rate. The excited waves are whistlers having comparatively long wavelength ($k\rho_e \simeq 0.06$ to 0.2) and small propagation angle ($\theta \simeq 33°$ to 55°). The electromagnetic and electrostatic components are comparable at low drift speeds, but the former becomes more dominant as the drift speed increases (Fig. 2b). Ion heating is expected since the free energy driving this instability comes from the ion drift. Electron heating is also anticipated as ξ_e (defined in A4) is small ($\lesssim 0.1$). Fig. 3 illustrates a substantial growth occurring over a broad range of θ (10° to 50°).

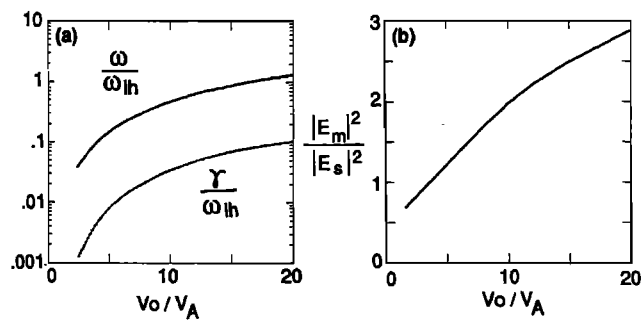

Figure 2. (a) Wave frequency and growth rate maximized over wavenumber and propagation angle as a function of the relative drift speed. (b) The ratio of electromagnetic to electrostatic components of the excited waves for the KCSI.

If the initiation of substorm expansion is due to the onset of KCSI in the neutral sheet and LHDI outside, then there are several implications which compare favorably with our present knowledge on the conditions under which substorm onset occurs. The instability growth and, presumably the resultant anomalous transport, is a strong function of the electron to ion drift. One possible way to enhance the relative drift between ions and electrons is by the cross-tail electric field since the unmagnetized ions undergo Speiser orbits and can be accelerated.

Under the above scenario, several observed features connected with substorm expansion onset can be accounted for by the proposed mechanism. The local time of substorm onset is known to be typically skewed towards the evening sector [e.g., Craven and Frank, 1989]. If the cross-tail electric field is the primary agent for increasing the relative drift, then it is natural to expect the highest speed attained by the unmagnetized ions to occur at the evening side of the thinned current sheet region in the midnight sector, perhaps even with ions making multiple neutral sheet encounters. Thus, the substorm onset is typically skewed towards the evening sector.

There are three conditions identified observationally which can trigger a substorm onset (see, e.g. Baumjohann, 1986), namely, (1) by northward turnings of the interplanetary magnetic field (IMF) during a southward IMF period, (2) by sudden enhancement of solar wind pressure, and (3) by an apparently internal process during steady southward IMF (with no identifiable onset signature in the solar wind). Substorms initiated by the first two conditions can be considered as being directly driven whereas those initiated by the third condition are due to unloading.

The first condition, suggested first by Rostoker [1983], can be understood in the following manner. During southward IMF, the auroral ovals expand, indicating an increase in the total magnetic flux content of the tail lobes. Assuming the tail lobe to be cylindrically symmetric, this increase in tail flux

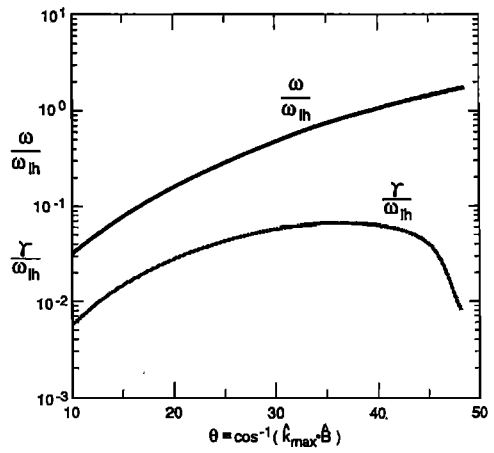

Figure 3. Wave frequency and growth rate, maximized over the wavenumber, as a function of the propagation angle for $v_o/v_A = 15$.

implies an induced electric field pointing dusk-to-dawn in the magnetotail current sheet, thus reducing the dawn-to-dusk electric field generated by the solar wind-magnetosphere dynamo. Therefore, northward turning of IMF at this time will decrease the opposing induced electric field, resulting in a sudden increase in the electric field in the dawn-to-dusk direction, which will in turn lead to an enhanced current sheet acceleration of ions in the neutral sheet to initiate the KCSI.

For the second triggering condition, it is observed that a sudden solar wind pressure enhancement leads to compression and thinning of the plasma sheet. This is accompanied by an enhanced dawn-to-dusk electric field which convects magnetotail plasma into the neutral sheet region, building up pressure in response to the larger external pressure. Again, the thinned plasma sheet leads to ions being unmagnetized in the neutral sheet and the enhanced electric field will increase the ion drift to drive the KCSI.

Finally, for the third triggering condition, it is well recognized from observations that both the cross-tail electric field and the B_z component in the neutral sheet (the two quantities that determine the amount of ion acceleration in the current sheet region) often exhibit large variations [Cattell and Mozer, 1987]. During southward IMF, it is very likely that these variations in localized regions of the current sheet can elevate the ion drift speed high enough to yield a favorable condition for the onset of the KCSI.

One can estimate the electric field strength required. The approximate energy gained from current sheet acceleration can be obtained by considering an ion executing a Speiser orbit and drifting in the direction of the electric field through a distance equal to twice its gyroradius. For a 2 keV ion, the gyroradius in an ambient magnetic field of 5 nT is about 1300 km. A relative drift speed of 1000 km/s ($\simeq 5\ v_A$) requires an acceleration of only 3.2 keV, corresponding to an averaged electric field strength of ~ 1 mV/m. A drift speed of 2000 km/s ($\simeq 10\ v_A$) requires an acceleration of 19 keV and an averaged electric field of ~ 7 mV/m. Electric fields of this strength and higher have been reported in the current sheet region during substorms [Cattell and Mozer, 1987]. Furthermore, the waves in the vicinity of the neutral sheet detected during substorms are found to have peak power at frequencies near the lower hybrid frequency as predicted by the instability analysis performed here.

Although the magnitude of current reduction by this instability has not been determined by non-linear analysis yet, we speculate here the plausible consequences. Magnetic stress and energy in the near-earth tail are enhanced by the gradual intensification of the cross-tail current prior to the substorm expansion. An abrupt current disruption can release the stress and energy in the tail with a collapse of highly stretched field lines into more dipolar field lines, resulting in a convection surge and auroral precipitation [Mauk, 1989]. Fermi acceleration (shortening of field lines) and betatron acceleration (field magnitude increase as a result of the collapse) are anticipated with this magnetic field change known as dipolarization. The turbulence due to LHDI outside the neutral sheet reduces the diamagnetic current (which is the energy source for LHDI) and therefore decreases the density gradient scale length. This leads to thickening of the plasma sheet, augmenting the thickening arising from dipolarization. Observations indeed show associated plasma sheet thickening.

Discussion and Conclusions

Numerical solutions to the linear dispersion equation of the kinetic cross-field streaming instability shows that this instability is a possible trigger for substorm expansions. The most probable onset location in the tail is where the strongest current flows, i.e. where the magnetic field configuration changes from dipolar to tail-like. Its growth can lead to a local current reduction, which forces part of the cross-tail current to continue through the ionosphere due to the large inductance of the current system. A current wedge is thus formed. However, if the ionospheric condition is not appropriate for the imposed current (see, e.g., the treatment by Kan et al., 1988), then the current diversion is impeded by the modification of magnetospheric electric fields through Alfvén waves bouncing between the two regions. A pseudo-breakup phenomenon may result instead.

The excited waves resulting from the instability have a mixed polarization with comparable electromagnetic and electrostatic components. Enhanced magnetic turbulence in the neutral sheet is therefore anticipated, consistent with in situ observations of current disruption [Lui et al., 1988]. The wave frequencies are in the lower hybrid frequency range, in agreement with observations also [Cattell and Mozer, 1987]. Heating is expected for both ions and electrons. The current disruption mechanism causes dipolarization which can energize particles further via Fermi and betatron acceleration.

The cross-tail electric field plays an important role in enhancing the relative drift between ions and electrons to drive the instability. Note that dipolarization is associated with an induced dawn-to-dusk electric field which will accelerate unmagnetized ions in adjacent regions and can lead to further spatial spreading of the unstable region in the neutral sheet. This corresponds to the local time widening of the substorm current wedge and radial spreading of the disturbance. The electric field magnitude needed to initiate the instability is within the range of electric fields often observed in the neutral sheet during substorm periods.

The scenario developed for substorm expansion onset based on this mechanism can readily account for the observed fact that the local time for substorm onset is typically skewed towards the evening sector from the midnight meridian. Furthermore, the three conditions in the solar wind under which substorm onset is observed can be understood.

Appendix

We outline here the dispersion equation used. For specie α (α = i or e), $T_\alpha = m_\alpha v_\alpha^2/2$ is the temperture, m_α is the mass, v_α is the thermal speed, $\Omega_\alpha = |e|B/m_\alpha$ is the gyrofrequency, $\rho_\alpha = v_\alpha/\Omega_\alpha$ is the gyroradius, n_α is the number density, β_α is the plasma beta, and $\omega_{p\alpha}$ is the plasma frequency. The electrons are taken to be magnetized while ions are unmagnetized. The equilibrium distribution functions for electrons and ions are Maxwellian with ions drifting at a velocity v_o perpendicular to the ambient magnetic field. Our analysis is performed in the guiding center rest frame of the electrons using the coordinate system in Figure 1. Taking the local approximation, neglecting the higher harmonic terms in the electron orbit integration, and considering waves

propagating in the yz-plane, i.e., $\mathbf{k} = k_\parallel \mathbf{B}/B + k_y \hat{e}_y$, we find the dispersion equation to be

$$1 + \chi_i(\omega,k) + \chi_{e,1}(\omega,k) + \chi_{e,2}(\omega,k) = 0. \quad \text{(A1)}$$

The first term in Eq. (A1) is the displacement current contribution, the second and third terms are electrostatic contributions from the ions and the electrons, respectively, and the last term contains the electromagnetic effects given as

$$\chi_{e,2}(\omega,k) = \frac{4\omega_{pe}^4}{k^4c^2v_e^2}\frac{D_1}{D_2}, \quad \text{(A2)}$$

where

$$D_1 = -\frac{4\omega_{pe}^2}{k^2c^2}\phi_2\phi_4\phi_5 + \phi_4^2\left[1 - \frac{\omega^2}{k^2c^2} + \frac{2\omega_{pe}^2}{k^2c^2}\phi_1\right] + \phi_2^2\left[1 - \frac{\omega^2}{k^2c^2} + \frac{2\omega_{pe}^2}{k^2c^2}\phi_6\right] + \frac{k_\parallel\omega}{k^2c}\left\{\frac{v_e}{c}\phi_2\phi_5 - \frac{k^2cv_e}{2\omega_{pe}^2}\phi_4\left[1 - \frac{\omega^2}{k^2c^2} + \frac{2\omega_{pe}^2}{k^2c^2}\phi_1\right]\right\},$$

$$D_2 = \left[1 - \frac{\omega^2}{k^2c^2} + \frac{2\omega_{pe}^2}{k^2c^2}\phi_6\right]\times\left[1 - \frac{\omega^2}{k^2c^2} + \frac{2\omega_{pe}^2}{k^2c^2}\phi_1\right] - \frac{4\omega_{pe}^4}{k^4c^4}\phi_5^2,$$

$$\phi_1 = -\xi_e\, Z(\xi_e)\mu e^{-\mu}[I_0(\mu) - I_1(\mu)],$$

$$\phi_2 = -(2\mu)^{-1/2}\phi_1,$$

$$\phi_3 = -\xi_e\, Z(\xi_e)e^{-\mu}I_0(\mu),\ \phi_4 = \frac{1 + \xi_e\, Z(\xi_e)}{Z(\xi_e)}\phi_3,$$

$$\phi_5 = \frac{1 + \xi_e\, Z(\xi_e)}{Z(\xi_e)}\phi_2,\ \phi_6 = \xi_e\,\phi_4, \quad \text{(A3)}$$

$$\xi_i = (\omega - k_y v_0)/kv_i,\ \xi_e = \frac{\omega}{k_\parallel v_e},\ \mu \simeq k_y^2v_e^2/2\Omega_e^2, \quad \text{(A4)}$$

$I_n(\mu)$ being the modified Bessel function of order n and $Z(\xi_e)$ being the plasma dispersion function.

Acknowledgment. This work was supported in part by NASA Grant NAG 5-759 to the Johns Hopkins University, Applied Physics Laboratory and in part by NASA Grant NAG 5-1101 and NASA Solar Terrestrial Theory Grant NAGW-971 to the University of Maryland.

References

Baumjohann, W., Some recent progress in substorm studies, *J. Geomag. Geoelectr., 38*, 633-651, 1986.

Cattell, C. A. and F. S. Mozer, Substorm-associated lower hybrid waves in the plasma sheet observed by ISEE-1, in *Magnetotail Physics*, ed. A. T. Y. Lui, Johns Hopkins University Press, Baltimore, p. 119-125, 1987.

Chang, C.-L., H.-K. Wong, Kinetic instabilities driven by cross-field ion streaming motion, *Trans. Amer. Geophys. Union, 70*, 1270, 1989.

Craven, J. D., and L. A. Frank, Diagnosis of auroral dynamics using global auroral imaging with emphasis on large-scale evolutions, in *Auroral Physics*, ed. by C.-I. Meng, Cambridge, England, 1990.

Coroniti, F. V., Explosive tail reconnection: the growth and expansion phases of magnetospheric substorms, *J. Geophys. Res., 90*, 7427-7448, 1985.

Huang, C. Y., C. K. Goertz, L. A. Frank, and G. Rostoker, Observational determination of the adiabatic index in the quiet time plasma sheet, *Geophys. Res. Lett., 16*, 563-566, 1989.

Huba, J. D., N. T. Gladd, K. Papadopoulos, Lower hybrid drift wave turbulence in the distant magnetotail, *J. Geophys. Res., 83*, 5217-5226, 1978.

Huba, J. D. and K. Papadopoulos, Non-linear stabilization of the lower hybrid drift instability by electron resonance broadening, *Phys. Fluids, 21*, 121-123, 1978.

Kan, J. R., L. Zhu, S.-I. Akasofu, A theory of substorms: onset and subsidence, *J. Geophys. Res., 93*, 5624-5640, 1988.

Kaufmann, R. L., Substorm currents: growth phase and onset, *J. Geophys. Res., 92*, 7471-7486, 1987.

Lui, At. T. Y., Estimates of current changes in the geomagnetotail associated with a substorm, *Geophys. Res. Lett., 5*, 853-856, 1978.

Lui, A. T. Y., et al., A case study of magnetotail current sheet disruption and diversion, *Geophys. Res. Lett., 15*, 721-724, 1988.

Mauk, B. H., Generation of macroscopic magnetic-field-aligned electric fields by the convection surge in acceleration mechanism, *J. Geophys. Res., 94*, 8911-8920, 1989.

Papadopoulos, K., The role of microturbulence on Collisionless Reconnection, in Dynamics of the Magnetosphere, ed. by S.-I. Akasofu, p. 289-309, 1979.

Rostoker, G., Triggering of expansive phase intensifications of magnetospheric substorms by northward turnings of the interplanetary magnetic field, *J. Geophys. Res., 88*, 6981-6993, 1983.

Speiser, T. W., Particle trajectories in model current sheets, 1, Analytical solutions, *J. Geophys. Res., 70*, 4219-4226, 1965.

Winske, D., M. Tanaka, C. S. Wu, and K. B. Quest, Plasma heating at collisionless shocks due to the kinetic cross-field streaming instability, *J. Geophys. Res., 90*, 123-136, 1985.

Wu, C. S., et al., A kinetic cross-field streaming instability, *Phys. Fluids, 26*, 1259-1267, 1983.

Wu, C. S., et al., Microinstabilities associated with a high Mach number perpendicular bow shock, *Space Sci. Rev., 37*, 63-109, 1984.

A. T. Y. Lui, Applied Physics Laboratory, John Hopkins University, Laurel, Maryland, 20723.

A. Mankofsky, C.-L. Chang, Science Applications International Corporation, McLean, Virginia, 20742.

K. Papadopoulos and C.S. Wu, Institute for Physical Science and Technology, University of Maryland, College Park, Maryland 20742

(Received November 10, 1989;
revised February 9, 1990;
accepted February 26, 1990)